ACCSCIENCE PUBLISHING

Eurasian Journal of Medicine and Oncology

ORIGINAL RESEARCH ARTICLE

Vitamin D/Vitamin D receptor signaling suppresses gastric cancer metastasis through autophagy-related protein 13/Beclin1-mediated autophagy

Jinrui Yang[1,2], Linyun Tan[3], Ruolin Shi[1,2], Qian Hu[1,2], Yinhong Gu[4], and Chao Du[1,2]*

[1]Institute of Biomedical Engineering, College of Medicine, Southwest Jiaotong University, Chengdu, Sichuan, China

[2]Department of Gastroenterology, The General Hospital of Western Theater Command, College of Medicine, Chengdu, Sichuan, China

[3]Department of Orthopedics, Orthopedic Research Institute, West China Hospital, Sichuan University, Chengdu, Sichuan, China

[4]Department of Clinical Medicine, College of Clinical Medicine, Chengdu Medical College, Chengdu, Sichuan, China

Abstract

Introduction: Gastric cancer (GC) exhibits a poor prognosis with high metastasis rates. This study investigates Vitamin D receptor's (VDRs) role in suppressing GC metastasis through autophagy.

Objective: To elucidate the molecular mechanism by which VDR suppresses GC invasion and metastasis through autophagy regulation.

Methods: VDR expression was assessed in 91 paired GC and adjacent normal tissues using immunohistochemistry. The effects of Vitamin D on GC cell proliferation, cell cycle, migration, and invasion were evaluated using Cell Counting Kit-8, flow cytometry, wound healing, and Transwell assays. The autophagic activity was examined through LysoTracker Red staining, monomeric red fluorescent protein-green fluorescent protein-LC3 fluorescence, and transmission electron microscopy. The roles of VDR, autophagy-related protein 13 (ATG13), and Beclin1 in autophagy regulation were investigated through gene knockdown and silencing. A nude mouse peritoneal metastasis model was used to validate the anti-metastatic effects of the Vitamin D/VDR pathway.

Results: VDR expression was significantly downregulated in GC tissues, correlating with lymph node metastasis and poor prognosis ($p<0.001$). Vitamin D treatment upregulated VDR, ATG13, and Beclin1 expression, enhancing autophagosome and autolysosome formation without altering cell proliferation or apoptosis, likely due to a cytostatic autophagic response. Silencing *ATG13* or *BECN1* abolished the inhibitory effects of Vitamin D/VDR signaling on cell migration and invasion. VDR knockdown promoted peritoneal metastasis, whereas Vitamin D treatment suppressed it.

Conclusion: This study provides novel evidence that Vitamin D/VDR signaling inhibits GC metastasis by influencing ATG13/Beclin1-mediated autophagy, offering potential therapeutic targets for GC management.

Keywords: Vitamin D signaling; Gastric cancer metastasis; Autophagy regulation; Vitamin D receptor; Autophagy-related protein 13; Beclin1

***Corresponding author:**
Chao Du
(dchaodoctor@foxmail.com)

Citation: Yang J, Tan L, Shi R, Hu Q, Gu Y, Du C. Vitamin D/Vitamin D receptor signaling suppresses gastric cancer metastasis through autophagy-related protein 13/Beclin1-mediated autophagy. *Eurasian J Med Oncol*. 2026;10(3):025150096. doi: 10.36922/EJMO025150096

Received: April 8, 2025

Revised: May 12, 2025

Accepted: May 22, 2025

Published online: August 13, 2025

1. Introduction

Gastric cancer (GC) remains a formidable global health challenge, ranking as the fifth most prevalent malignancy and the fourth leading cause of cancer-related mortality worldwide.[1] In China, the burden is particularly pronounced, with elevated incidence and mortality rates, compounded by a troubling increase in early-onset GC over the past three decades.[2,3] The disease's dismal prognosis stems primarily from its asymptomatic progression in early stages, which often delays diagnosis until therapeutic options are limited. In addition, the molecular complexity of GC—driven by the intricate interplay among genetic, environmental, and lifestyle factors—complicates the development of effective targeted treatments.[4] Consequently, there is an urgent need to identify novel molecular targets and unravel their regulatory mechanisms to enhance GC management and patient outcomes.

The Vitamin D receptor (VDR), a ligand-activated nuclear transcription factor, has garnered attention for its multifaceted roles in cancer biology. When bound to its active ligand, 1,25-dihydroxyvitamin D3 (VD), VDR heterodimerizes with the retinoid X receptor to regulate the expression of genes governing cell proliferation, apoptosis, and differentiation.[5,6] Interestingly, Vitamin D treatment itself can upregulate VDR expression through a positive feedback mechanism, wherein activated VDR binds to Vitamin D response elements located in distant enhancer regions within its gene locus, enhancing VDR transcription and amplifying the cellular response to Vitamin D.[7] This regulatory loop has been documented in various cell types and may contribute to tissue-specific responses to Vitamin D signaling.[8] Accumulating evidence underscores VDR's tumor-suppressive potential across various malignancies, including prostate, breast, and colorectal cancers.[9-14] In the context of GC, VDR gene polymorphisms, such as the *FokI* variant, have been linked to heightened cancer susceptibility,[14,15] while reduced VDR expression correlates with adverse prognostic outcomes.[16,17] Despite these associations, the precise mechanisms by which VDR modulates GC progression, particularly its metastatic behavior, remain insufficiently explored.

Autophagy, a highly conserved lysosomal degradation pathway, exerts a dual influence on cancer dynamics. During early tumorigenesis, autophagy suppresses malignant transformation by maintaining cellular homeostasis and removing damaged components. In contrast, in advanced cancers, it can bolster tumor cell survival, invasion, and metastasis by enhancing metabolic resilience under stress.[18,19] In GC, autophagy has been implicated in promoting metastasis through processes such as epithelial–mesenchymal transition and anoikis resistance.[20,21] Emerging research has begun to illuminate the interplay between VDR signaling and autophagy in cancer. For example, in breast cancer, VDR activation curtails pro-survival autophagy through the inositol-requiring enzyme 1α-c-Jun N-terminal kinase pathway,[22] whereas in non-small cell lung cancer, Vitamin D triggers a cytostatic autophagy that sensitizes cells to radiation.[23] However, the specific role of VDR-mediated autophagy regulation in GC metastasis remains a critical knowledge gap.

This study aims to investigate the role of VDR in modulating autophagy and its impact on GC metastasis. By employing a combination of clinical data analysis, *in vitro* assays, and *in vivo* models, we explored the potential of the VDR-autophagy axis as a therapeutic target for GC.

2. Materials and methods

2.1. Clinical specimen collection and ethics statement

GC tissues and adjacent normal tissues were obtained from 91 patients who underwent surgical resection at the General Hospital of Western Theater Command between January 2015 and December 2020. None of the patients received preoperative chemotherapy or radiotherapy. Demographic and clinicopathological data were collected from medical records. The study was approved by the Medical Ethics Committee of Western Theater Command General Hospital (Approval no. 2022EC4-ky010). Written informed consent was obtained from all patients before sample collection in accordance with the Declaration of Helsinki. Tissue specimens were fixed in 10% neutral-buffered formalin and embedded in paraffin for immunohistochemical analysis. Pathological staging was performed according to the 8th edition of the AJCC Cancer Staging Manual.[24]

2.2. Cell lines and culture

Human GC cell lines (SGC7901, MKN45) and normal gastric epithelial cell line (GES-1) were obtained from the Cell Bank of the Chinese Academy of Sciences (China). SGC7901 and MKN45 were specifically selected for functional experiments due to their established reliability in GC metastasis research, excellent transfection efficiency, and distinct differentiation states (moderately and poorly differentiated, respectively). All cell lines were authenticated using short tandem repeat profiling and tested for mycoplasma contamination every 3 months. Cells were maintained in Roswell Park Memorial Institute 1640 medium (11875093, Gibco, USA supplemented with 10% (v/v) fetal bovine serum (FBS; 10099141, Gibco, USA), 100 U/mL penicillin and 100 μg/mL streptomycin (15140122, Gibco, US) in a humidified incubator at 37°C

with 5% (v/v) carbon dioxide. Cells were passaged every 2 – 3 days using 0.25% (w/v) trypsin-ethylenediamine tetraacetic acid (25200056, Gibco, USA) until 80 – 90% confluence was reached. All experiments were performed using cells between passages 5 and 15.

2.3. Reagents and antibodies

1,25-dihydroxyvitamin D3 (D1530) was purchased from Sigma Aldrich (Germany). The concentrations of 1 μM and 5 μM were selected based on published literature and preliminary experiments showing optimal VDR pathway activation without cytotoxicity.[23,25] Primary antibodies against VDR (12550; 1:1,000), microtubule-associated protein 1 light chain 3B (LC3B; 3868; 1:1,000), p62 (88588; 1:1,000), autophagy-related protein 13 (ATG13; 13468; 1:1,000), Beclin1 (3495; 1:1,000), and glyceraldehyde-3-phosphate dehydrogenase (GAPDH; 5174; 1:5,000) were obtained from Cell Signaling Technology (USA). Horseradish peroxidase-conjugated anti-rabbit immunoglobulin (Ig)G (7074; 1:5,000) and anti-mouse IgG (7076; 1:5,000) secondary antibodies were from Cell Signaling Technology (USA).

2.4. Cell viability assay

Cell viability was assessed using Cell Counting Kit-8 (CCK-8; CK04, Dojindo, Japan). Cells were seeded in 96-well plates at a density of 5×10^3 cells/well in 100 μL complete medium and allowed to adhere overnight. Cells were then treated with different concentrations of VD (1 and 5 μmol/L) for 24 and 48 h. After treatment, 10 μL of CCK-8 reagent was added to each well and incubated for 2 h at 37°C. The absorbance was measured at 450 nm using a microplate reader (Multiskan FC, Thermo Scientific, USA). Cell viability was calculated as the percentage relative to untreated control cells. Each experiment was performed in sextuplicate and repeated 3 times independently.

2.5. Flow cytometry analysis

For cell cycle analysis, cells were harvested and fixed in 70% (v/v) ice-cold ethanol overnight at 4°C. Fixed cells were washed twice with phosphate-buffered saline and stained with propidium iodide solution containing 50 μg/mL propidium iodide (P4170, Sigma, Germany) and 100 μg/mL RNase A (R6513, Sigma, Germany) for 30 min at 37°C in the dark. For apoptosis analysis, cells were harvested and stained with phycoerythrin Annexin V Apoptosis Detection Kit (559763, BD Biosciences, USA) according to the manufacturer's instructions. Briefly, cells were resuspended in 100 μL binding buffer containing 5 μL of Annexin V-phycoerythrin and 5 μL of 7-Aminoactinomycin D, followed by 15 min incubation at room temperature in the dark. Flow cytometric analysis was performed using a BD FACSCanto II flow cytometer (BD Biosciences, USA). A minimum of 1×10^4 events were collected for each sample. Data were analyzed using the FlowJo software (version 10.0, Tree Star, USA).

2.6. Migration assays

For the wound healing assay, cells were seeded in 6-well plates and grown to 90% confluence. A sterile 200 μL pipette tip was used to create a straight scratch across the cell monolayer. Floating cells were removed by washing twice with phosphate-buffered saline, and a fresh medium containing 2% (v/v) FBS was added. Images of the wounds were captured at 0 h and 24 h using an Olympus IX73 inverted microscope (Japan) at ×100 magnification. The wound closure distance was measured using ImageJ software (version 1.53) and calculated as in Equation I:

$$([\text{initial width} - \text{final width}]/\text{initial width}) \times 100\% \quad \text{(I)}$$

For the Transwell migration assay, 2×10^4 cells in 200 μL serum-free medium were seeded into the upper chamber of the Transwell inserts (8 μm pore size, 3422, Corning, USA). The lower chamber was filled with 600 μL medium containing 10% (v/v) FBS as a chemoattractant. After 24 h of incubation, non-migrated cells on the upper surface were gently removed using cotton swabs. Migrated cells on the lower surface were fixed with 4% (w/v) paraformaldehyde for 15 min and stained with 0.1% (w/v) crystal violet for 15 min at room temperature. Five random fields per insert were photographed under a microscope (×200 magnification), and cells were counted using the ImageJ software. Each experiment was performed in triplicate and repeated three times independently.

2.7. Lentiviral infection and small interfering RNA transfection

Lentiviral short hairpin (sh)RNA targeting *VDR* (5'-GCAGATCCTAATCGACTTCAT-3') and control shRNA were constructed and packaged by Lilai Biomedicine (China). Cells were infected with lentivirus in the presence of 8 μg/mL polybrene (TR-1003, Sigma, Germany). Stable cell lines were selected using 2 μg/mL puromycin (P8833, Sigma, Germany) for a week. For transient knockdown, small interfering (si)RNAs targeting *ATG13 (*5'-GCAGTTGGAACAGGCTGAAAT-3') and *BECN1 (*5'-GCCTGGACCGTGTCACCATTT-3') were synthesized by Lilai Biomedicine and transfected using Lipofectamine 3000 (L3000015, Invitrogen, USA) according to the manufacturer's instructions.

2.8. Autophagy detection

For LysoTracker Red staining, cells grown on coverslips were incubated with 50 nmol/L LysoTracker Red DND-99

(L7528, Invitrogen, USA) for 30 min at 37°C. Cells were then fixed with 4% (w/v) paraformaldehyde, counterstained with 1 μg/mL of 4',6-diamidino-2-phenylindole (D9542, Sigma, Germany), and mounted using a ProLong Glass Antifade Mountant (P36982, Invitrogen, USA). Images were acquired using a Leica SP8 confocal microscope (Germany) with a ×63 oil immersion objective.

For autophagic flux analysis, cells were transfected with a monomeric red fluorescent protein-green fluorescent protein-LC3 (mRFP-GFP-LC3) plasmid (84572, Addgene, USA) using Lipofectamine 3000 (L3000015, Invitrogen, USA) according to the manufacturer's protocol. After 24 h of transfection, cells were treated with 100 nmol/L of 1,25(OH)2D3 for 24 h. Fluorescence images were captured using a Leica SP8 confocal microscope (Germany). For quantitative analysis of the mRFP-GFP-LC3 assay, at least 30 cells per condition were randomly selected from three independent experiments. Yellow puncta (autophagosomes) and red-only puncta (autolysosomes) were counted using ImageJ software. For transmission electron microscopy (TEM), cells were fixed with 2.5% (v/v) glutaraldehyde in 0.1 mol/L phosphate buffer (pH 7.4) for 2 h at 4°C, post-fixed with 1% (w/v) osmium tetroxide for an hour, and dehydrated through a graded ethanol series (30%, 50%, 70%, 80%, 90%, 95%, and 100% [v/v]). Samples were embedded in Epon 812 resin and polymerized at 60°C for 48 h. Ultrathin sections (70 nm) were prepared using a Leica EM UC7 ultramicrotome (Germany), stained with uranyl acetate and lead citrate, and examined using a JEM-1400Plus transmission electron microscope (JEOL, Japan) at an accelerating voltage of 80 kV.

2.9. Western blot analysis

Total protein was extracted using ice-cold radioimmunoprecipitation assay buffer (P0013B, Beyotime, China) containing protease inhibitor cocktail (04693159001, Roche, Switzerland) and phosphatase inhibitor cocktail (04906845001, Roche, Switzerland). Protein concentration was determined using the BCA Protein Assay Kit (23225, Thermo Scientific, USA). Equal amounts of protein (30 μg/lane) were separated by sodium dodecyl sulfate-polyacrylamide gel electrophoresis on 10 – 12% gels at 80 V for 30 min, followed by 120 V for 90 min. Proteins were transferred onto 0.45 μm polyvinylidene fluoride membranes (IPVH00010, Millipore, USA) at 300 mA for 90 min at 4°C. Membranes were blocked with 5% (w/v) non-fat milk in Tris-buffered saline with Tween 20 (TBST; 20 mmol/L^{-1} Tris-hydrochloric acid [pH 7.4], 150 mmol/L sodium chloride, 0.1% [v/v] Tween 20) for an hour at room temperature.

Membranes were incubated with primary antibodies overnight at 4°C: anti-VDR (1:1,000; 12550, Cell Signaling Technology, USA), anti-LC3B (1:1,000; 3868, Cell Signaling Technology, USA), anti-p62 (1:1,000; 88588, Cell Signaling Technology, USA), anti-ATG13 (1:1,000; 13468, Cell Signaling Technology, USA), anti-Beclin1 (1:1000; 3495, Cell Signaling Technology, USA), and anti-GAPDH (1:5,000, 5174, Cell Signaling Technology, USA). After washing 3 times with TBST (10 min each), membranes were incubated with horseradish peroxidase-conjugated secondary antibodies (1:5,000; 7074 or 7076, Cell Signaling Technology, USA) for an hour at room temperature. Protein bands were visualized using enhanced chemiluminescence reagent (WBKLS0500, Millipore, USAFun) and detected using the ChemiDoc XRS+ imaging system (Bio-Rad, USA). Band intensities were quantified using ImageJ software and normalized to GAPDH.

2.10. RNA extraction and quantitative polymerase chain reaction (PCR)

Total RNA was extracted using TRIzol reagent (15596026, Invitrogen, USA) following the manufacturer's protocol. RNA concentration and purity were determined using the NanoDrop 2000 spectrophotometer (Thermo Scientific, USA), with an A260/A280 ratio between 1.8 and 2.0 considered acceptable. RNA integrity was assessed using 1% agarose gel electrophoresis. Complementary DNA was synthesized from 1 μg of total RNA using the PrimeScript RT reagent Kit (RR037A, Takara, USA) according to the manufacturer's instructions. Quantitative PCR (qPCR) was performed using the SYBR Green Master Mix (4309155, Applied Biosystems, USA) on an ABI 7500 Real-Time PCR system (Applied Biosystems, USA). The primers used were as follows:

(i) *VDR*: Forward 5'-GCCCACCATAAGACCTACGA-3'
Reverse 5'-AGATTGGAGAAGCTGGACGA-3'
(ii) *ATG5*: Forward 5'-AAAGATGTGCTTCGAGAT GTGT-3'
Reverse 5'-CACTTTGTCAGTTACCAACGTCA-3'
(iii) *ATG7*: Forward 5'-ATGATCCCTGTAACTTAGC CCA-3'
Reverse 5'-CACGGAAGCAAACAACTTCAAC-3'
(iv) *ATG13*: Forward 5'-CTGTTCCTGGAGTTTCTG GAC-3'
Reverse 5'-AGGTGTCATCATACTTCTCATCC-3'
(v) *ATG14*: Forward 5'-GCTTCGAAGGTCACACA TCG-3'
Reverse 5'-TCCTGGTTGTGCTGCTACTG-3'
(vi) *BECN1*:Forward5'-CCATGCAGGTGAGCTTCGT-3'
Reverse 5'-GAATCTGCGAGAGACACCATC-3'
(vii) *GAPDH*: Forward 5'-GGAGCGAGATCCCTCCAA AAT-3'
Reverse 5'-GGCTGTTGTCATACTTCTCATGG-3'

The PCR reactions were carried out in a 20 μL volume containing 10 μL of SYBR Green Master Mix, 0.8 μL each of forward and reverse primers (10 μmol/L), 2 μL of complementary DNA template, and 6.4 μL of nuclease-free water. The cycling conditions were: initial denaturation at 95°C for 10 min, followed by 40 cycles of 95°C for 15 s and 60°C for 1 min. Melting curve analysis was performed to confirm reaction specificity. *GAPDH* served as the internal control. Relative gene expression was calculated using the $2^{-\Delta\Delta CT}$ method. All reactions were performed in triplicate.

2.11. Animal studies

Female BALB/c nude mice (6 weeks old, 18 – 20 g, total used: 32) were purchased from Shanghai Model Organisms Center, Inc. (China). Mice were housed under specific pathogen-free conditions with controlled temperature (22 ± 2°C), humidity (55 ± 5%), and 12-h light/dark cycles. After 1 week of acclimatization, mice were randomly divided into experimental groups (n = 5 per group). SGC7901 cells (5×10^6) stably expressing control or VDR shRNA were injected intraperitoneally. For VD treatment, mice received VD (21 IU/kg) or vehicle by intraperitoneal injection 3 times/week. Body weight was monitored weekly. After 4 months, mice were sacrificed by cervical dislocation under anesthesia, and peritoneal metastatic nodules were counted. Serum calcium levels were measured using a Beckman Coulter AU5800 (Beckman Coulter, USA) automatic biochemical analyzer. All animal procedures were approved by the Medical Ethics Committee of Western Theater Command General Hospital (Approval no. 2022EC4-ky010) and conducted in accordance with institutional guidelines for animal care and welfare.

2.12. Statistical analysis

Statistical analyses were performed using GraphPad Prism 8.0 software. Data are presented as mean ± standard error of the mean from at least three independent experiments. Two-tailed Student's *t*-test was used for comparisons between the two groups. One-way analysis of variance followed by Tukey's *post hoc* test was used for multiple comparisons. Survival curves were analyzed using the Kaplan–Meier plot database (https://kmplot.com/analysis/). A value of $p<0.05$ was considered statistically significant.

3. Results

3.1. Downregulation of VDR in GC correlates with lymph node metastasis and poor prognosis

To investigate the potential role of VDR in GC pathogenesis, we initially examined VDR protein expression in 91 pairs of GC specimens and their adjacent non-cancerous tissues.

Immunohistochemical analysis revealed robust VDR expression predominantly localized in normal gastric epithelial tissues, while matched GC specimens exhibited markedly diminished immunoreactivity (Figure 1A). Quantitative assessment confirmed significantly reduced VDR expression in GC tissues compared to adjacent normal tissues ($p<0.001$; Figure 1F). Immunofluorescence analysis further characterized VDR's subcellular distribution, demonstrating both nuclear and perinuclear localization in GC cells (Figure 1B), consistent with VDR's known function as a nuclear transcription factor with cytoplasmic-nuclear shuttling capability.

To determine the clinical significance of VDR downregulation, we analyzed correlations between VDR expression and key clinicopathological parameters. While VDR expression showed no significant association with gender (Figure 1C) or tumor size (Figure 1D), reduced VDR levels were significantly correlated with lymph node metastasis ($p<0.05$; Figure 1E) and advanced TNM stage (III/IV) ($p<0.01$, Figure 1L). These associations suggest that VDR downregulation may contribute to GC progression rather than initiation.

Kaplan–Meier survival analysis using the KMplot database revealed that patients with high VDR expression exhibited significantly better clinical outcomes across multiple survival metrics, including overall survival (hazard ratio [HR] = 0.67, 95% confidence interval [CI]: 0.56 – 0.79), post-progression survival (HR = 0.65, 95% CI: 0.52 – 0.82), and progression-free survival (HR = 0.68, 95% CI: 0.56 – 0.83) (all $p<0.001$; Figure 1G-J). The consistent prognostic value of VDR across these parameters reinforces its potential tumor suppressive function in GC.

To validate these clinical findings at the cellular level, we examined VDR protein expression across multiple GC cell lines compared to the normal gastric epithelial cell line, GES-1. Western blot analysis demonstrated consistently decreased VDR protein levels in GC cell lines (Figure 1K), with quantitative densitometry confirming significant downregulation ($p<0.01$). This cell-based evidence corroborates our tissue-based observations, collectively suggesting that diminished VDR expression may represent a key molecular alteration in GC pathogenesis.

3.2. Vitamin D/VDR axis inhibits GC cell invasion and migration without affecting cell proliferation and survival

To characterize the biological effects of Vitamin D on GC cells, we first assessed its impact on cellular proliferation and viability. CCK-8 assay revealed that treatment with Vitamin D (1 μM and 5 μM) for 24 and 48 h did not significantly influence the viability of either normal

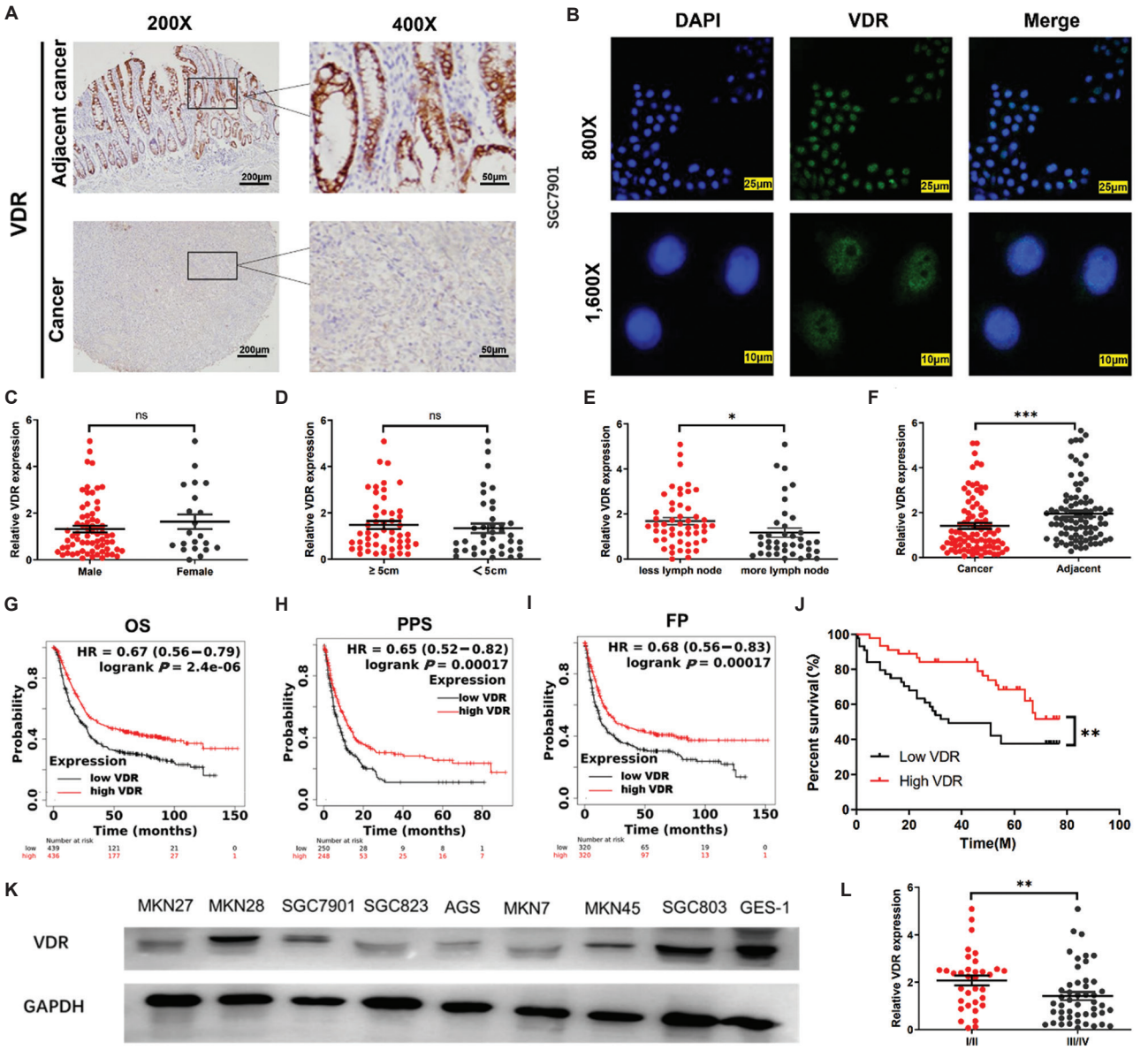

Figure 1. Downregulation of Vitamin D receptor (VDR) in gastric cancer (GC) correlates with lymph node metastasis and poor prognosis. (A) Representative immunohistochemical staining of VDR in gastric cancer and adjacent normal tissues (n = 91). Scale bars: 50 μm and 200 μm, magnifications: ×200 and ×400. (B) Immunofluorescence showing VDR localization (green) in SGC7901 cells. Nuclei counterstained with DAPI (blue). Scale bars: 20 μm and 10 μm, magnifications: ×800 and ×1,600. (C-E) VDR expression in GC samples stratified by (C) sex, (D) tumor size, and (E) lymph node metastasis. (F) Quantitative analysis of VDR expression in GC versus adjacent tissues (n = 91). (G-J) Kaplan–Meier survival analyses of GC patients by VDR expression: (G) overall survival, (H) post-progression survival, (I) progression-free survival, and (J) integrated analysis from the KMplot database. (K) Western blot of VDR expression in normal gastric epithelial cells and GC cell lines. GAPDH served as the loading control. (L) VDR expression correlation with TNM stages.

Notes: Statistical significance at $^{*}p<0.05$, $^{**}p<0.01$, and $^{***}p<0.001$. ns refers to not significant.

Abbreviations: DAPI: 4',6-diamidino-2-phenylindole; HR: Hazard ratio; GAPDH: Glyceraldehyde-3-phosphate dehydrogenase.

gastric epithelial cells (GES-1) or GC cells (MKN45) (Figure 2A and B). Flow cytometry analysis of cell cycle distribution (Figure 2C) and apoptosis (Figure 2D and E) further confirmed that Vitamin D treatment had no significant effect on GC cell proliferation or survival.

Subsequently, we investigated whether Vitamin D treatment affected VDR expression in GC cells. Western blot analysis demonstrated that VDR protein levels increased progressively in both SGC7901 and MKN45 cells following Vitamin D (1 μM) treatment in a time-dependent

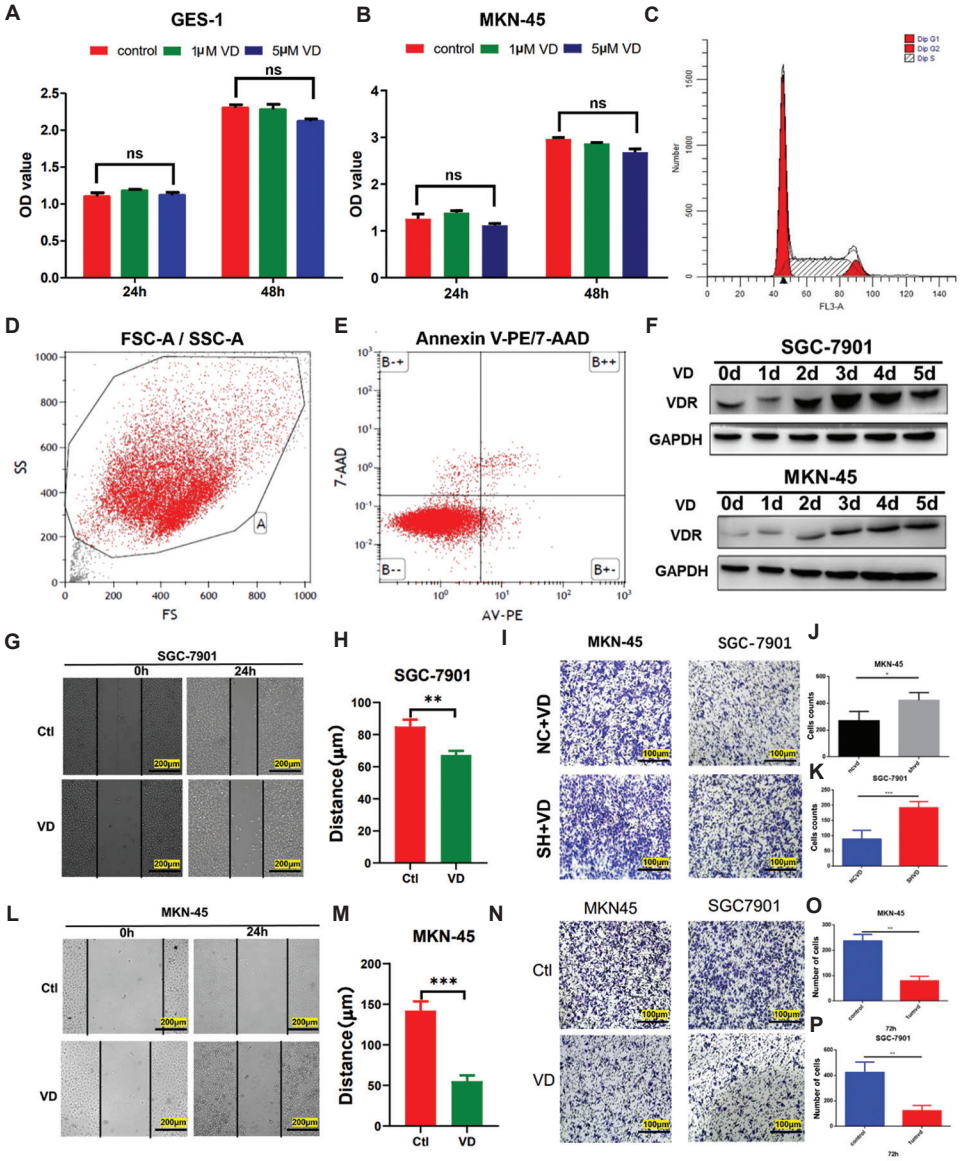

Figure 2. Vitamin D inhibits gastric cancer cell migration through VDR signaling without affecting proliferation or survival. (A and B) Cell Counting Kit-8 assay demonstrating that VD treatment (1 μM and 5 μM) for 24 and 48 h had no significant effect on cell viability in (A) normal gastric epithelial cells and (B) gastric cancer cells (MKN45). (C) Flow cytometry analysis of cell cycle distribution in MKN45 cells after 24 h of VD (1 μM) treatment. (D-E) Apoptosis assessment by flow cytometry showing (D) FSC/SSC gating strategy and (E) representative Annexin V-PE/7-AAD dot plots indicating no significant apoptotic induction by VD treatment. (F) Western blot analysis revealing time-dependent upregulation of VDR protein expression in SGC7901 and MKN45 cells treated with VD (1 μM) for 0 – 5 days. GAPDH served as the loading control. (G and H) Wound healing assay in SGC7901 cells with (G) representative micrographs at 0 and 24 h and (H) quantification of wound closure distance. (I and J) Wound healing assay in MKN45 cells with (I) representative micrographs at 0 and 24 h and (J) quantification of wound closure distance. Scale bar: 100 μm, magnification: ×100. (K-M) Transwell migration assay showing (K) representative images of migrated cells and quantification of migrated cell numbers for (L) MKN45 and (M) SGC7901 cells, respectively. Scale bar: 100 μm, magnification: ×200. (N-P) VDR knockdown attenuates VD-mediated migration inhibition. (N) Representative images of migrated cells in control short hairpin (sh)RNA (NC+VD) and VDR shRNA (shVDR+VD) groups. (O-P) Quantification of migrated cell numbers in both cell lines.

Notes: Statistical significance at $*p<0.05$, $**p<0.01$, and $***p<0.001$. ns refers to not significant.

Abbreviations: AAD: Aminoactinomycin D; Ctl: Control; FSC: Forward scatter; GAPDH: Glyceraldehyde-3-phosphate dehydrogenase; OD: Optical density; PE: Phycoerythrin; SSC: Side scatter; VD: 1,25-dihydroxyvitamin D3; VDR: Vitamin D receptor.

manner (Figure 2F). This finding indicates that Vitamin D effectively upregulates its cognate receptor in GC cells.

To determine the functional consequences of Vitamin D-induced VDR upregulation, we examined its effects

on GC cell migration. A wound healing assay revealed that Vitamin D significantly suppressed the migratory capacity of GC cells. Vitamin D-treated SGC7901 cells exhibited significantly reduced wound closure compared to untreated controls (p<0.01; Figure 2G and H). Similar inhibitory effects were observed in MKN45 cells (p<0.001; Figure 2L and M). These observations were further corroborated by the Transwell migration assay, which demonstrated a marked reduction in the number of migrating cells following Vitamin D treatment in both cell lines (Figure 2N-P).

To establish the role of VDR in mediating Vitamin D's anti-migratory effects, we generated VDR-knockdown GC cells using shRNA. Notably, in VDR-deficient cells, the inhibitory effect of Vitamin D (1 μM) on cell migration was significantly attenuated (Figure 2I-K). This finding provides compelling evidence that Vitamin D suppresses GC cell migration, specifically through VDR activation.

Collectively, these results demonstrate that Vitamin D selectively inhibits the invasive and migratory potential of GC cells through VDR signaling, without affecting cellular proliferation or survival mechanisms.

3.3. Vitamin D promotes autophagy in GC cells through the VDR signaling pathway

To elucidate the molecular mechanism by which the VD/VDR signaling pathway inhibits GC invasion and metastasis, we first investigated the effect of VD treatment on autophagic activity in GC cells. LysoTracker Red staining revealed a significant increase in acidic vesicular organelles in both MKN45 and SGC7901 GC cells following treatment with VD (100 nM, 24 h) compared to the control group (Figure 3A). To further confirm autophagic flux, we employed the mRFP-GFP-LC3 dual fluorescence reporting system, which demonstrated that VD treatment markedly enhanced the formation of autophagosomes (yellow fluorescent puncta) and autolysosomes (red fluorescent puncta) (Figure 3B). Quantitative analysis confirmed that VD treatment significantly increased both autophagosome and autolysosome formation in SGC7901 and MKN45 cells compared to control groups (p<0.01; Figure 3H). This quantitative data provides robust evidence for VD-induced enhancement of autophagic flux in GC cells (Figure 3H). TEM analysis further corroborated these findings, showing characteristic double-membrane autophagosomes in VD-treated cells (Figure 3D, red arrows), whereas no obvious autophagic structures were observed in the control group.

Western blot analysis demonstrated that VD treatment induced a time-dependent increase in VDR expression, accompanied by an elevated LC3B-II/I ratio and decreased p62 levels (Figure 3E and F), all of which are hallmarks of autophagy activation. To further delineate the role of VDR in VD-induced autophagy, we established VDR-knockdown GC cell lines. As shown in Figure 3G, VDR silencing significantly reduced the LC3B-II/I ratio, while LysoTracker Red staining also showed markedly diminished autophagic activity in VDR-knockdown cells (Figure 3C). These results indicate that VD can promote autophagic activity in GC cells through upregulation of VDR expression.

3.4. Vitamin receptor D knockdown promotes *in vivo* metastasis of GC cells

To directly assess the impact of VDR on GC metastasis *in vivo*, we established stable VDR knockdown (VDR-shRNA) and control (VDR-NC) SGC7901 cells for xenograft transplantation in nude mice. As shown in Figure 4A, compared with the control group, the VDR knockdown group demonstrated significantly increased peritoneal metastatic nodules (p<0.01; Figure 4B). Furthermore, mice in the VDR knockdown group exhibited a marked reduction in body weight (p<0.01; Figure 4E), suggesting increased tumor burden.

To verify the safety and autophagy-activating effects of VD treatment *in vivo*, mice were administered low-dose VD (21 IU/kg). Results showed that this dosage had no significant impact on serum calcium levels or body weight (Figure 4C and D), indicating that the therapeutic dose was safe and reliable. Concurrently, western blot analysis revealed that VD treatment significantly upregulated the expression of VDR and LC3B-II/I in gastric tissues (Figure 4F), confirming that VD could similarly promote autophagy through VDR *in vivo*. These results suggest that VDR plays an inhibitory role in GC metastasis *in vivo*, and VD treatment may suppress GC metastasis by enhancing autophagy.

3.5. Vitamin D/VDR signaling inhibits GC metastasis through ATG 13 and Beclin1-mediated autophagy

To elucidate the molecular mechanism by which VD/VDR signaling inhibits GC metastasis, we performed a qPCR analysis. Results revealed that VD treatment significantly upregulated the expression of multiple autophagy-related genes, including *ATG5*, *ATG7*, *ATG13*, *ATG14*, and *BECN1* (p<0.01 or ***p<0.001, Figure 5A-F), while *ATG3*, *ATG12*, and *ULK1* expression showed no significant changes (Figure 5G-I). Western blot analysis further confirmed these alterations at the protein level (Figure 5J), and notably, VDR knockdown markedly reduced the expression of these ATGs (Figure 5K).

To further validate the functional roles of ATG13 and Beclin1 in the VD/VDR signaling pathway, we established

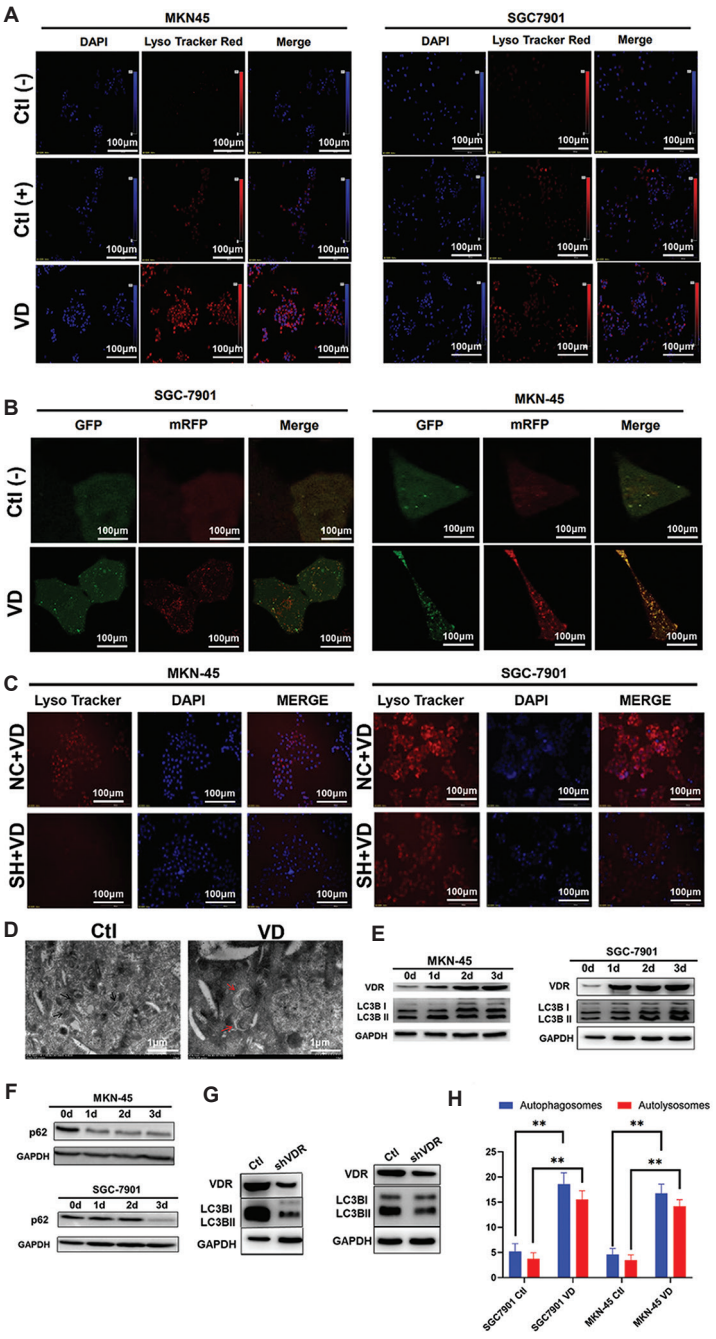

Figure 3. Vitamin D promotes autophagy through Vitamin D receptor (VDR) activation in gastric cancer cells. (A) LysoTracker Red staining in MKN45 and SGC7901 cells with or without VD treatment (100 nM, 24 h). DAPI: blue. Scale bar: 100 μm, magnification: ×400. (B) mRFP-GFP-LC3 reporter assay in SGC7901 and MKN45 cells. Yellow puncta: autophagosomes, red puncta: autolysosomes. Scale bar: 100 μm, magnification: ×400. (C) LysoTracker Red staining in control (NC+VD) and VDR-knockdown (SH+VD) cells treated with VD. Scale bar: 100 μm, magnification: ×400. (D) Transmission electron microscopy images of control and VD-treated cells. Red arrows indicate double-membrane autophagosomes. Scale bars: 1 μm (left), 0.5 μm (right). Magnifications: ×10,000 (left), ×20,000 (right). (E) Western blot of VDR and LC3B-I/II expression in cells treated with VD (100 nM) for 0 – 3 days. (F) Western blot of p62 expression in cells treated with VD over time. (G) Western blot showing LC3B-II/I ratio in control and VDR-knockdown cells. GAPDH served as the loading control. (H) Quantification of autophagosomes (blue) and autolysosomes (red) in control and VD-treated cells. Data are presented as mean ± SEM from 30 cells per condition.

Note: Statistical significance determined at $^{**}p<0.01$.

Abbreviations: Ctl: Control; DAPI: 4',6-diamidino-2-phenylindole; GAPDH: Glyceraldehyde-3-phosphate dehydrogenase; LC3B: Microtubule-associated protein 1 light chain 3B; mRFP-GFP-LC3: Monomeric red fluorescent protein-green fluorescent protein-LC3; SEM: Standard error of mean; SH: Short hairpin; VD: 1,25-dihydroxyvitamin D3.

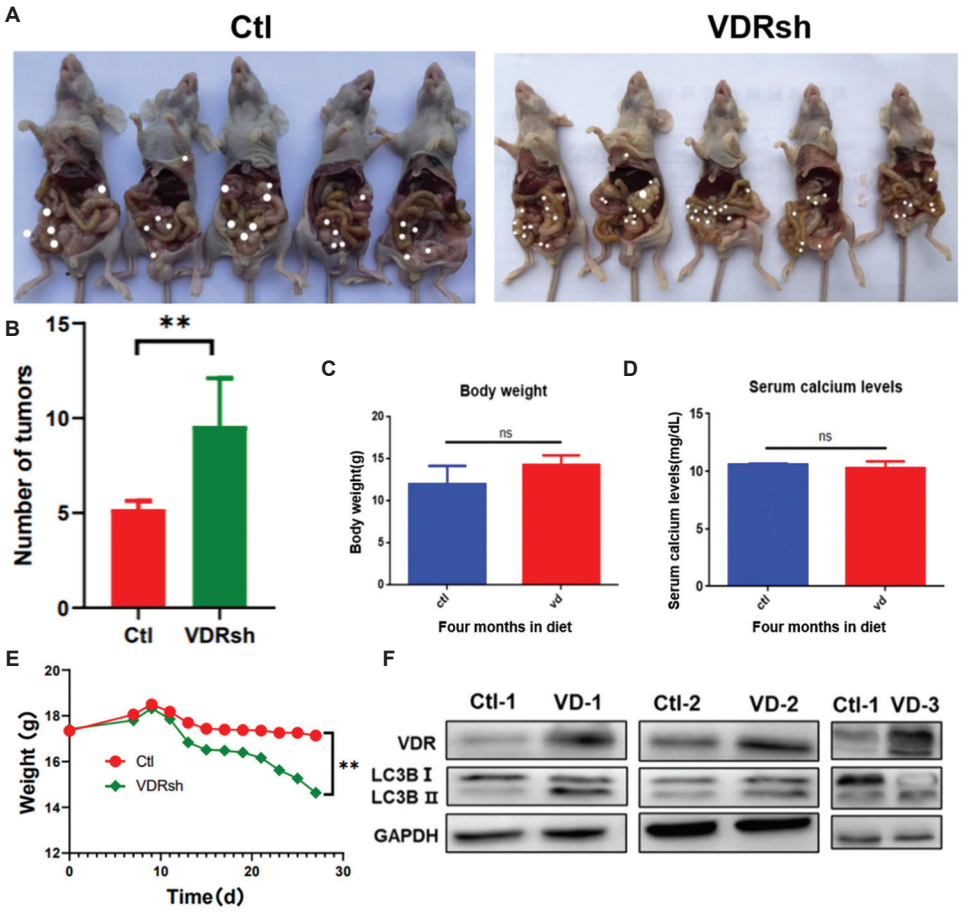

Figure 4. Vitamin D receptor knockdown promotes gastric cancer metastasis *in vivo*, while VD treatment safely activates autophagy. (A) Representative images showing increased peritoneal metastatic nodules (white dots) in nude mice implanted with VDR-knockdown (VDRsh) SGC7901 cells compared to control cells. (B) Quantification of peritoneal metastatic nodules ($n = 5$ mice per group). (C) Body weight and (D) serum calcium levels remained unchanged in mice after VD treatment (21 IU/kg) for 4 months. (E) Body weight curves of mice monitored over 30 days after implantation showing significant weight loss in the VDR knockdown group. (F) Western blot showing increased VDR and LC3B-I/II expression in gastric tissues from VD-treated mice compared to controls. GAPDH served as the loading control.

Note: Statistical significance determined at $^{**}p<0.01$. ns refers to not significant.

Abbreviations: Ctl: Control; GAPDH: Glyceraldehyde-3-phosphate dehydrogenase; LC3B: Microtubule-associated protein 1 light chain 3B; VD: 1,25-dihydroxyvitamin D3.

ATG13 and *BECN1* knockdown GC cell models using siRNA technology. Knockdown efficiency was confirmed by qPCR (Figure 5L-O) and Western blot analysis (Figure 5P-S). Functional studies demonstrated that silencing either *ATG13* or *BECN1* significantly enhanced the migration capacity of both SGC7901 and MKN45 GC cells ($p<0.001$; Figure 6A-F), indicating that these autophagy-related genes play crucial roles in suppressing GC invasion and metastasis. Multiple independent replicate experiments further validated these findings (Figure 6G-L).

Collectively, these results demonstrate that the VD/VDR signaling pathway inhibits GC invasion and metastasis by upregulating ATG13 and Beclin1-mediated autophagy, thereby providing potential novel therapeutic targets for GC treatment.

4. Discussion

In this study, we have elucidated a novel molecular mechanism by which the Vitamin D/VDR signaling pathway suppresses GC invasion and metastasis through autophagy regulation. We demonstrated that VDR expression is significantly downregulated in GC tissues and correlates with patient prognosis. Across both *in vitro* and *in vivo* experiments, we established that Vitamin D upregulates VDR expression, thereby activating autophagy through ATG13 and Beclin1-mediated pathways, ultimately inhibiting the invasive and metastatic capabilities of GC

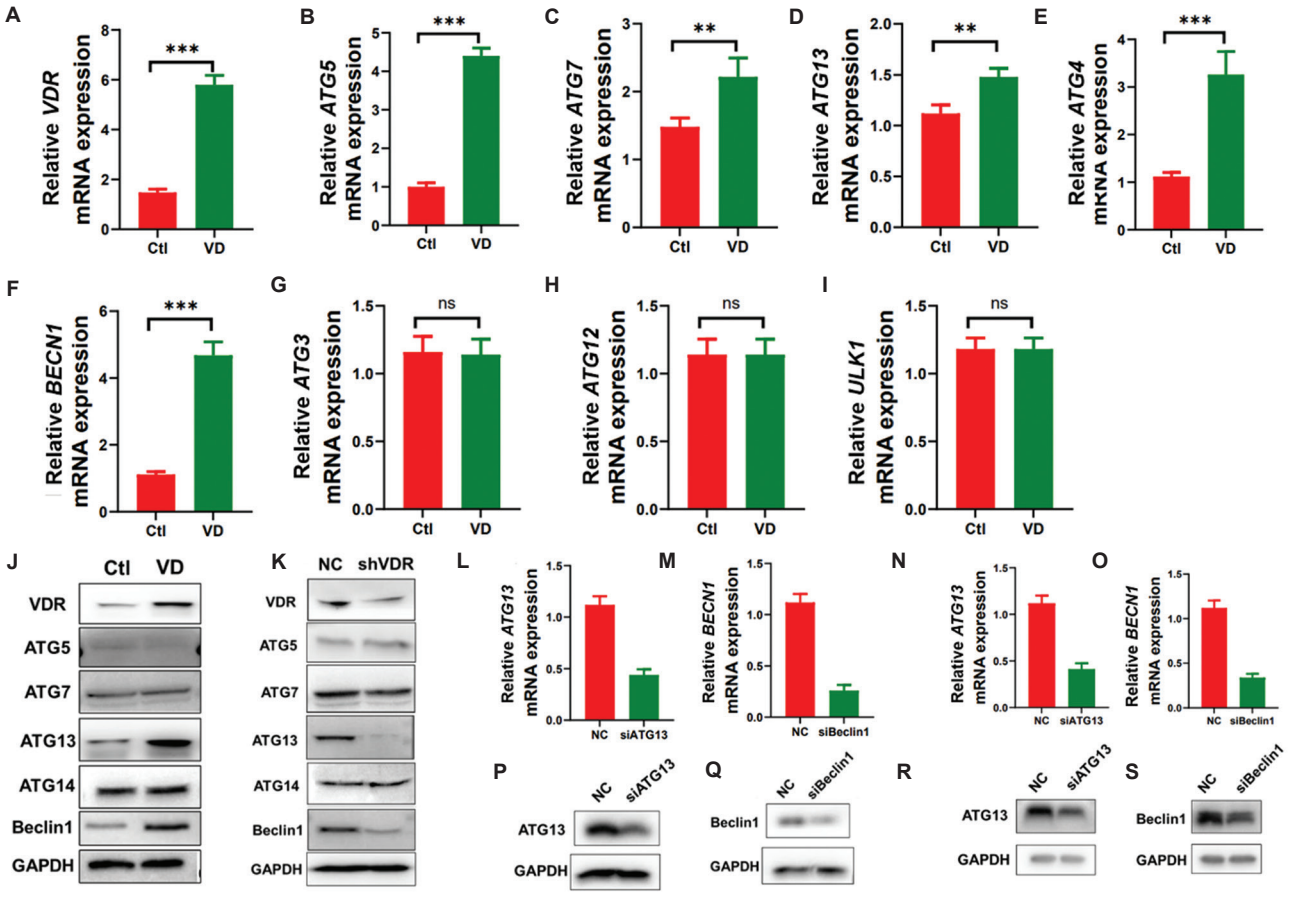

Figure 5. Vitamin D upregulates autophagy-related genes through the Vitamin D receptor, while the knockdown of *ATG13* or *BECN1* abolishes this effect. (A-I) qPCR analysis showing expression of autophagy-related genes in GC cells after VD treatment (100 nM, 24 h). VD significantly upregulated mRNA levels of (A) *VDR*, (B) *ATG5*, (C) *ATG7*, (D) *ATG13*, (E) *ATG14*, and (F) *BECN1*, while (G) *ATG3*, (H) *ATG12*, and (I) *ULK1* showed no significant changes. (J) Western blot showing increased protein levels of VDR and autophagy-related proteins after VD treatment. (K) Western blot confirming that VDR knockdown reduced the expression of autophagy-related proteins. (L-O) qPCR validation of *ATG13* and *BECN1* knockdown efficiency in SGC7901 and MKN45 cells. (P-S) Western blot confirmation of successful ATG13 and Beclin1 protein knockdown. GAPDH served as the loading control for all Western blot analyses.

Note: Statistical significance determined at $^{**}p<0.01$ and $^{***}p<0.001$. ns refers to not significant.

Abbreviations: ATG13: Autophagy-related protein 13; Ctl: Control; GAPDH: Glyceraldehyde-3-phosphate dehydrogenase; NC: Normal control; qPCR: Quantitative polymerase chain reaction; sh: Short hairpin; VD: 1,25-dihydroxyvitamin D3.

cells. These findings not only expand our understanding of Vitamin D's antitumor mechanisms but also provide potential therapeutic strategies for GC treatment.

Initially, our clinical sample analysis revealed significantly reduced VDR expression in GC tissues, with expression levels negatively correlating with lymph node metastasis and TNM stage. The observed variations in VDR expression among different GC cell lines likely reflect their distinct genetic backgrounds and differentiation states, while all consistently showing downregulation compared to normal gastric epithelium.[26,27] Survival analysis demonstrated that patients with high VDR expression exhibited better overall survival and progression-free survival, suggesting VDR as a potential prognostic indicator for GC. These findings align with a recent Cancer Genome Atlas database analysis by Zhang *et al.*,[28] which identified a significant correlation between VDR expression and GC patient survival. Multiple epidemiological studies have established that Vitamin D deficiency is closely associated with increased GC risk and poor prognosis.[29] Moreover, extensive research has documented that VDR polymorphisms significantly correlate with GC susceptibility across different populations.[30,31]

In exploring VDR's functional mechanism, we found that Vitamin D treatment significantly enhanced VDR expression in GC cells without affecting cell proliferation or apoptosis. This observation differs from Chen *et al.*'s findings,[32] who reported Vitamin D-mediated inhibition

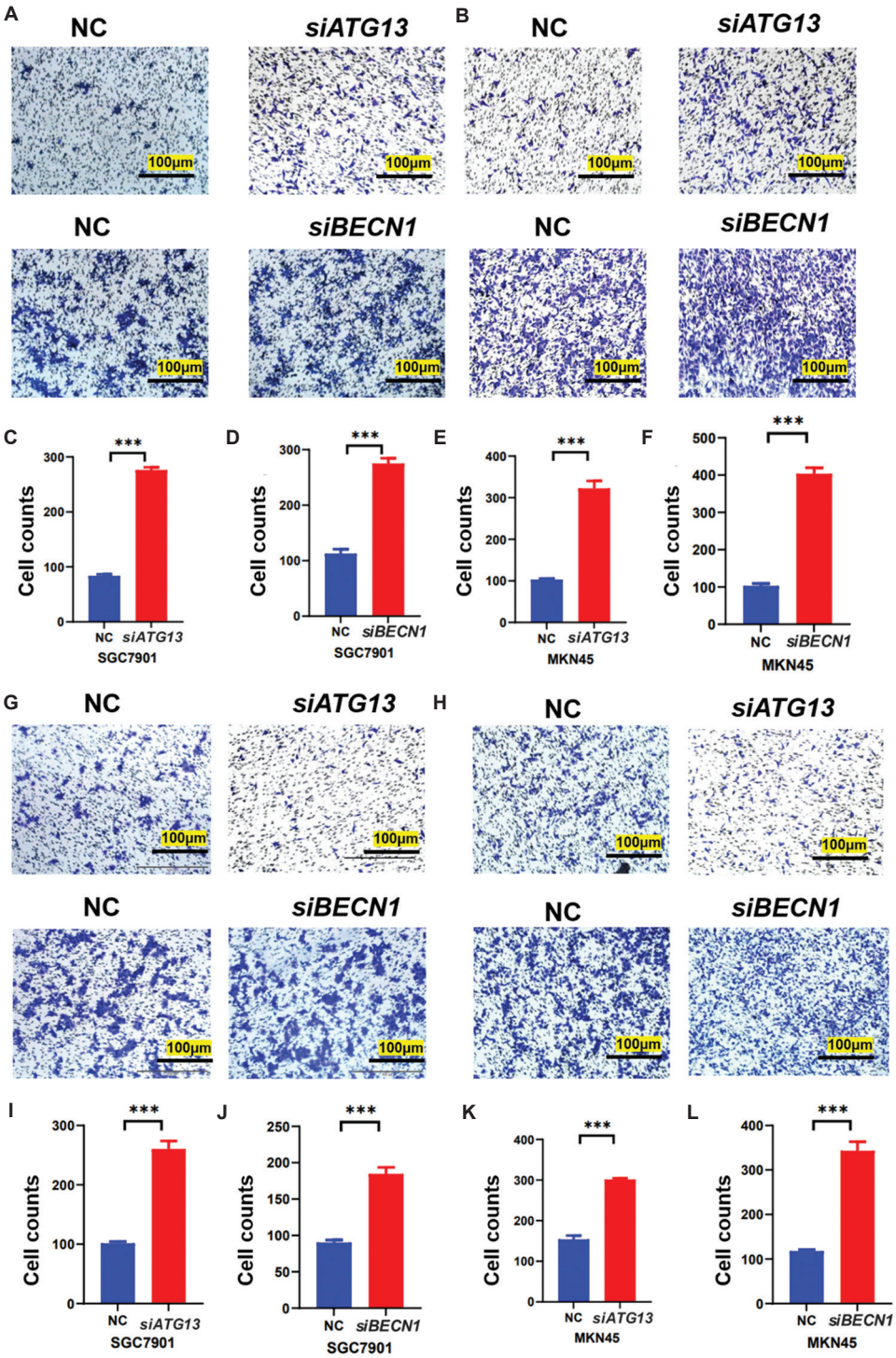

Figure 6. Silencing of *ATG13* or *BECN1* enhances gastric cancer cell migration capability. (A and B) Representative images of Transwell migration assays showing increased migration in (A) SGC7901 and (B) MKN45 cells after *ATG13* or *BECN1* knockdown. Scale bar: 100 μm, magnification: ×200. (C-F) Quantification of migrated cells in (C and D) SGC7901 and (E and F) MKN45 cells after *ATG13* or *BECN1* knockdown. (G-L) Independent replicate experiments confirming enhanced migration capacity in both cell lines following *ATG13* or *BECN1* knockdown: (G-J) SGC7901 cells and (K-L) MKN45 cells. Scale bar: 100 μm, magnification: ×200. Data are presented as mean ± SEM from three independent experiments.

Note: Statistical significance determined at ***$p<0.001$.

Abbreviations: Ctl: Control; NC: Normal control; qPCR: Quantitative polymerase chain reaction; si: Small interfering.

of tumor cell proliferation. This discrepancy may be attributed to variations in tumor types and experimental conditions. Notably, we observed that VDR activation markedly suppressed GC cell migration and invasion. Further investigation revealed that this inhibitory effect was achieved through autophagy regulation. Recent studies have demonstrated the complex roles of autophagy in tumor metastasis. For instance, autophagy-mediated metabolic reprogramming significantly enhances tumor cell metastatic potential in non-small cell lung cancer,[33] while in melanoma, autophagy plays a crucial role in tumor microenvironment remodeling and metastatic niche formation.[34] It is important to note that the role of autophagy in cancer progression is highly context-dependent. Numerous studies have documented this context-dependent duality of autophagy in cancer. For example, Kimmelman and White[35] demonstrated that autophagy promotes tumor growth by maintaining cellular metabolism and providing tumors with metabolic plasticity in harsh microenvironments, while autophagy in early tumorigenesis suppresses cancer development by eliminating damaged organelles and reducing genomic instability, thereby preventing oxidative stress conducive to DNA damage.[35,36] In GC specifically, Zhang *et al*.[37] reported that high mobility group box 1-induced autophagy promotes chemoresistance and tumor growth by activating the receptor for advanced glycation end products-extracellular signal-regulated kinases 1/2 pathway, whereas Qin *et al*.[38] found that autophagy inhibition promotes epithelial–mesenchymal transition and metastasis by altering the metabolic phenotype in GC cells. The seemingly paradoxical effects of autophagy – tumor-suppressive in some contexts while tumor-promoting in others – may be reconciled by considering the stage-specific functions of autophagy and the nature of autophagic response. In our study, VD appeared to induce cytostatic rather than cytotoxic autophagy in GC cells, which selectively inhibited cellular invasion without affecting proliferation. This type of autophagy differs from canonical survival autophagy by restricting cellular plasticity required for metastatic processes, including epithelial–mesenchymal transition and anoikis resistance.[39,40] Understanding this mechanistic distinction may be crucial for developing autophagy-modulating strategies in GC therapy.

At the molecular level, we identified ATG13 and Beclin1 as key targets of Vitamin D/VDR signaling in autophagy regulation. In breast cancer, Li *et al*.[22] demonstrated that VDR activation attenuates pro-survival autophagy through the inositol-requiring enzyme 1α-c-Jun N-terminal kinase pathway. In cervical cancer, Vitamin D enhances radiosensitivity by suppressing Ambra1-mediated autophagy.[41] Our study uniquely demonstrates that Vitamin D treatment significantly upregulates autophagy-related genes, including *ATG5*, *ATG7*, *ATG13*, *ATG14*, and *BECN1*. Notably, *ATG13*, as an essential component of the *ULK1* complex, plays a critical role in autophagy initiation. We found that knockdown of either *ATG13* or *BECN1* significantly attenuated Vitamin D's inhibitory effects on GC cell migration and invasion, consistent with observations in non-small cell lung cancer where Vitamin D induces cytostatic autophagy through VDR and p53-dependent mechanisms.[23] The molecular mechanisms by which VDR regulates ATG13 and Beclin1 expression likely involve direct transcriptional regulation. As a ligand-activated transcription factor, VDR may bind to Vitamin D response elements (VDREs) in the promoter regions of these autophagy-related genes. Indeed, bioinformatic analysis reveals putative VDRE sequences in both *ATG13* and *BECN1* promoters.[25] Alternatively, VDR might regulate these genes indirectly through intermediate transcription factors, such as forkhead box O3 or through epigenetic modifications of their promoter regions.[42] Future chromatin immunoprecipitation and promoter activity assays are needed to elucidate the precise regulatory mechanisms.

Animal studies further validated the crucial role of the Vitamin D/VDR/autophagy axis in suppressing GC metastasis. We observed that VDR knockdown significantly promoted the peritoneal metastasis of GC cells, while Vitamin D treatment exhibited inhibitory effects on metastasis. Importantly, the Vitamin D dosage (21 IU/kg) used in our study did not induce hypercalcemia, suggesting a favorable safety profile.[43] Recent clinical studies have also demonstrated that Vitamin D supplementation can improve cancer patient outcomes with minimal adverse effects.[44]

However, several limitations in our study warrant further investigation. First, the precise molecular mechanism by which VDR influences *ATG13* and *BECN1* transcription remains to be fully elucidated. While our results suggest a regulatory relationship, future studies employing chromatin immunoprecipitation and promoter analysis would further clarify whether this regulation occurs through direct VDR binding or through intermediate signaling pathways. Second, the crosstalk between the Vitamin D/VDR pathway and other autophagy regulatory pathways requires further exploration. In addition, the clinical efficacy of Vitamin D analogs needs to be validated through prospective studies.

Future research directions should focus on:

(i) Zinvestigating the detailed molecular mechanisms of Vitamin D/VDR signaling in autophagy regulation,
(ii) developing more effective VDR agonists, and

(iii) evaluating the combination of Vitamin D analogs with existing therapeutic strategies. Our findings provide new insights into GC metastasis prevention and treatment, with significant potential for clinical translation.

5. Conclusion

We demonstrated that Vitamin D suppresses GC metastasis through VDR-mediated autophagy activation. Mechanistically, our evidence indicates that VDR signaling enhances ATG13 and Beclin1 expression to promote autophagy, thereby inhibiting cancer cell invasion. These findings reveal a novel Vitamin D/VDR/autophagy regulatory axis in GC progression and suggest potential therapeutic strategies.

Acknowledgments

The authors would like to take this opportunity to express our sincere gratitude to Southwest Jiaotong University for their strong support of this research.

Funding

This work was supported by the Military Medical Science and Technology Youth Program (Grant No. 21QNPY121) and the National Natural Science Foundation of China (Grant No. 81702931).

Conflict of interest

The authors declare no conflict of interest.

Author contributions

Conceptualization: Jinrui Yang
Data curation: Ruolin Shi, Qian Hu
Formal analysis: Linyun Tan, Yinhong Gu
Investigation: Jinrui Yang, Linyun Tan, Ruolin Shi, Qian Hu
Methodology: Jinrui Yang
Writing – original draft: Jinrui Yang
Writing – review & editing: Chao Du

Ethics approval and consent to participate

All animal procedures were approved by the Medical Ethics Committee of Western Theater Command General Hospital (Approval No. 2022EC4-ky010) and conducted in accordance with institutional guidelines for animal care and welfare. For clinical samples, written informed consent was obtained from all patients before sample collection in accordance with the Declaration of Helsinki.

Consent for publication

Written informed consent for publication was obtained from all participants.

Availability of data

The datasets used and/or analyzed during the present study are available from the corresponding author on reasonable request.

References

AQ5

1. Sung H, Ferlay J, Siegel RL, *et al*. Global cancer statistics 2020: GLOBOCAN estimates of incidence and mortality worldwide for 36 cancers in 185 countries. *CA Cancer J Clin*. 2021;71(3):209-249.

   doi: 10.3322/caac.21660

2. Cao W, Chen HD, Yu YW, Li N, Chen WQ. Changing profiles of cancer burden worldwide and in China: A secondary analysis of the global cancer statistics 2020. *Chin Med J (Engl)*. 2021;134(7):783-791.

   doi: 10.1097/cm9.0000000000001474

3. He Y, Wang Y, Luan F, *et al*. Chinese and global burdens of gastric cancer from 1990 to 2019. *Cancer Med*. 2021;10(10):3461-3473.

   doi: 10.1002/cam4.3892

4. Seeneevassen L, Bessède E, Mégraud F, Lehours P, Dubus P, Varon C. Gastric cancer: Advances in carcinogenesis research and new therapeutic strategies. *Int J Mol Sci*. 2021;22(7):3418.

   doi: 10.3390/ijms22073418

5. Haussler MR, Whitfield GK, Kaneko I, *et al*. Molecular mechanisms of vitamin D action. *Calcif Tissue Int*. 2013;92(2):77-98.

   doi: 10.1007/s00223-012-9619-0

6. Pike JW, Meyer MB. Fundamentals of vitamin D hormone-regulated gene expression. *J Steroid Biochem Mol Biol*. 2014;144 Pt A:5-11.

   doi: 10.1016/j.jsbmb.2013.11.004

7. Zella LA, Kim S, Shevde NK, Pike JW. Enhancers located within two introns of the vitamin D receptor gene mediate transcriptional autoregulation by 1,25-dihydroxyvitamin D3. *Mol Endocrinol*. 2006;20(6):1231-1247.

   doi: 10.1210/me.2006-0015

8. Haussler MR, Whitfield GK, Haussler CA, *et al*. The nuclear vitamin D receptor: Biological and molecular regulatory properties revealed. *J Bone Miner Res*. 1998;13(3):325-349.

   doi: 10.1359/jbmr.1998.13.3.325

9. Li H, Stampfer MJ, Hollis JB, *et al*. A prospective study of plasma vitamin D metabolites, vitamin D receptor polymorphisms, and prostate cancer. *PLoS Med*. 2007;4(3):e103.

   doi: 10.1371/journal.pmed.0040103

10. Gross M, Kost SB, Ennis B, Stumpf W, Kumar R. Effect

of 1,25-dihydroxyvitamin D3 on mouse mammary tumor (GR) cells: Evidence for receptors, cellular uptake, inhibition of growth and alteration in morphology at physiologic concentrations of hormone. *J Bone Miner Res.* 1986;1(5):457-467.

doi: 10.1002/jbmr.5650010510

11. Moossavi M, Parsamanesh N, Mohammadoo-Khorasani M, *et al*. Positive correlation between vitamin D receptor gene FokI polymorphism and colorectal cancer susceptibility in South-Khorasan of Iran. *J Cell Biochem*. 2018;119(10):8190-8194.

doi: 10.1002/jcb.26826

12. Xu Y, He B, Pan Y, *et al*. Systematic review and meta-analysis on vitamin D receptor polymorphisms and cancer risk. *Tumour Biology.* 2014;35(5):4153-4169.

doi: 10.1007/s13277-013-1544-y

13. Gnagnarella P, Pasquali E, Serrano D, Raimondi S, Disalvatore D, Gandini S. Vitamin D receptor polymorphism FokI and cancer risk: A comprehensive meta-analysis. *Carcinogenesis*. 2014;35(9):1913-1619.

doi: 10.1093/carcin/bgu150

14. Chen WY, Bertone-Johnson ER, Hunter DJ, Willett WC, Hankinson SE. Associations between polymorphisms in the vitamin D receptor and breast cancer risk. *Cancer Epidemiol Biomarkers Prev*. 2005;14(10):2335-2339.

doi: 10.1158/1055-9965.Epi-05-0283

15. Bid HK, Kumar A, Kapoor R, Mittal RD. Association of vitamin D receptor-gene (FokI) polymorphism with calcium oxalate nephrolithiasis. *J Endourol*. 2005;19(1):111-115.

doi: 10.1089/end.2005.19.111

16. Jurutka PW, Whitfield GK, Hsieh JC, Thompson PD, Haussler CA, Haussler MR. Molecular nature of the vitamin D receptor and its role in regulation of gene expression. *Rev Endocr Metab Disord*. 2001;2(2):203-216.

doi: 10.1023/a:1010062929140

17. Colin EM, Weel AE, Uitterlinden AG, *et al*. Consequences of vitamin D receptor gene polymorphisms for growth inhibition of cultured human peripheral blood mononuclear cells by 1, 25-dihydroxyvitamin D3. *Clin Endocrinol (Oxf)*. 2000;52(2):211-216.

doi: 10.1046/j.1365-2265.2000.00909.x

18. Galluzzi L, Pietrocola F, Bravo-San Pedro JM, *et al*. Autophagy in malignant transformation and cancer progression. *EMBO J*. 2015;34(7):856-880.

doi: 10.15252/embj.201490784

19. Debnath J, Gammoh N, Ryan KM. Autophagy and autophagy-related pathways in cancer. *Nat Rev Mol Cell Biol*. 2023;24(8):560-575.

doi: 10.1038/s41580-023-00585-z

20. Li W, Zhou C, Yu L, *et al*. Tumor-derived lactate promotes resistance to bevacizumab treatment by facilitating autophagy enhancer protein RUBCNL expression through histone H3 lysine 18 lactylation (H3K18la) in colorectal cancer. *Autophagy*. 2024;20(1):114-130.

doi: 10.1080/15548627.2023.2249762

21. Dong Y, Jin Q, Sun M, *et al*. CLDN6 inhibits breast cancer metastasis through WIP-dependent actin cytoskeleton-mediated autophagy. *J Exp Clin Cancer Res.* 2023;42(1):68.

doi: 10.1186/s13046-023-02644-x

22. Li Y, Cook KL, Yu W, *et al*. Inhibition of antiestrogen-promoted pro-survival autophagy and tamoxifen resistance in breast cancer through vitamin D receptor. *Nutrients*. 2021;13(5):1715.

doi: 10.3390/nu13051715

23. Sharma K, Goehe RW, Di X, *et al*. A novel cytostatic form of autophagy in sensitization of non-small cell lung cancer cells to radiation by vitamin D and the vitamin D analog, EB 1089. *Autophagy*. 2014;10(12):2346-2361.

doi: 10.4161/15548627.2014.993283

24. Amin MB, Greene FL, Edge SB, *et al*. The eighth edition AJCC cancer staging manual: Continuing to build a bridge from a population-based to a more "personalized" approach to cancer staging. *CA Cancer J Clin*. 2017;67(2):93-99.

doi: 10.3322/caac.21388

25. Tavera-Mendoza LE, Westerling T, Libby E, *et al*. Vitamin D receptor regulates autophagy in the normal mammary gland and in luminal breast cancer cells. *Proc Natl Acad Sci U S A*. 2017;114(11):E2186-E2194.

doi: 10.1073/pnas.1615015114

26. Gao JP, Xu W, Liu WT, Yan M, Zhu ZG. Tumor heterogeneity of gastric cancer: From the perspective of tumor-initiating cell. *World J Gastroenterol*. 2018;24(24):2567-2581.

doi: 10.3748/wjg.v24.i24.2567

27. Ho SWT, Tan P. Dissection of gastric cancer heterogeneity for precision oncology. *Cancer Sci*. 2019;110(11):3405-3414.

doi: 10.1111/cas.14191

28. Zhang Y, Li Y, Wei Y, Cong L. Molecular mechanism of vitamin D receptor modulating wnt/β-catenin signaling pathway in gastric cancer. *J Cancer*. 2023;14(17):3285-3294.

doi: 10.7150/jca.81034

29. Wen Y, Da M, Zhang Y, Peng L, Yao J, Duan Y. Alterations in vitamin D signaling pathway in gastric cancer progression: A study of vitamin D receptor expression in human normal, premalignant, and malignant gastric tissue. *Int J Clin Exp Pathol*. 2015;8(10):13176-13184.

30. Parsamanesh N, Moossavi M, Tavakkoli T, *et al*. Positive

correlation between vitamin D receptor gene TaqI variant and gastric cancer predisposition in a sample of Iranian population. *J Cell Physiol*. 2019;234(9):15044-15047.

doi: 10.1002/jcp.28145

31. Cong L, Wang WB, Liu Q, Du JJ. FokI polymorphism of the vitamin D receptor gene is associated with susceptibility to gastric cancer: A case-control study. *Tohoku J Exp Med*. 2015;236(3):219-224.

doi: 10.1620/tjem.236.219

32. Chen Y, Du J, Zhang Z, *et al*. MicroRNA-346 mediates tumor necrosis factor α-induced downregulation of gut epithelial vitamin D receptor in inflammatory bowel diseases. *Inflamm Bowel Dis*. 2014;20(11):1910-1918.

doi: 10.1097/mib.0000000000000158

33. Wang J, Gong M, Fan X, Huang D, Zhang J, Huang C. Autophagy-related signaling pathways in non-small cell lung cancer. *Mol Cell Biochem*. 2022;477(2):385-393.

doi: 10.1007/s11010-021-04280-5

34. Pangilinan C, Klionsky DJ, Liang C. Emerging dimensions of autophagy in melanoma. *Autophagy*. 2024;20(8):1700-1711.

doi: 10.1080/15548627.2024.2330261

35. Kimmelman AC, White E. Autophagy and tumor metabolism. *Cell Metab*. 2017;25(5):1037-1043.

doi: 10.1016/j.cmet.2017.04.004

36. Kung CP, Budina A, Balaburski G, Bergenstock MK, Murphy M. Autophagy in tumor suppression and cancer therapy. *Crit Rev Eukaryot Gene Expr*. 2011;21(1):71-100.

doi: 10.1615/critreveukargeneexpr.v21.i1.50

37. Zhang QY, Wu LQ, Zhang T, Han YF, Lin X. Autophagy-mediated HMGB1 release promotes gastric cancer cell survival via RAGE activation of extracellular signal-regulated kinases 1/2. *Oncol Rep*. 2015;33(4):1630-1638.

doi: 10.3892/or.2015.3782

38. Qin W, Li C, Zheng W, *et al*. Inhibition of autophagy promotes metastasis and glycolysis by inducing ROS in gastric cancer cells. *Oncotarget*. 2015;6(37):39839-39854.

doi: 10.18632/oncotarget.5674

39. Onorati AV, Dyczynski M, Ojha R, Amaravadi RK. Targeting autophagy in cancer. *Cancer*. 2018;124(16):3307-3318.

doi: 10.1002/cncr.31335

40. Gugnoni M, Sancisi V, Manzotti G, Gandolfi G, Ciarrocchi A. Autophagy and epithelial-mesenchymal transition: An intricate interplay in cancer. *Cell Death Dis*. 2016;7(12):e2520.

doi: 10.1038/cddis.2016.415

41. Zhang Z, Yu X, Cheng G. Vitamin D sensitizes cervical cancer to radiation-induced apoptosis by inhibiting autophagy through degradation of ambra1. *Cell Death Discov*. 2025;11(1):1.

doi: 10.1038/s41420-024-02279-7

42. Seuter S, Neme A, Carlberg C. Epigenome-wide effects of vitamin D and their impact on the transcriptome of human monocytes involve CTCF. *Nucleic Acids Res*. 2016;44(9):4090-4104.

doi: 10.1093/nar/gkv1519

43. DeSmet ML, Fleet JC. Constitutively active RAS signaling reduces 1,25 dihydroxyvitamin D-mediated gene transcription in intestinal epithelial cells by reducing vitamin D receptor expression. *J Steroid Biochem Mol Biol*. 2017;173:194-201.

doi: 10.1016/j.jsbmb.2017.01.008

44. Manson JE, Cook NR, Lee IM, *et al*. Vitamin D supplements and prevention of cancer and cardiovascular disease. *N Engl J Med*. 2019;380(1):33-44.

doi: 10.1056/NEJMoa1809944